Supporting information

Lattice capacity-dependent activity for CO_2 methanation: Crafting Ni/CeO_2 catalysts with outstanding performance at low temperatures

Kun Liu[b, *], Yixin Liao[a], Peng Wang[c], Xiuzhong Fang[a], Jia Zhu[d], Guangfu Liao [e, *]
Xianglan Xu[a, *]

[a] Key Laboratory of Jiangxi Province for Environment and Energy Catalysis, Institute of Rare Earths, School of Chemistry and Chemical Engineering, Nanchang University, Nanchang, Jiangxi 330031, China

[b] School of Resources and Environment, Nanchang University, 999 Xuefu Road, Nanchang, Jiangxi, 330031, China

[c] Shandong Chambroad Petrochemicals Co., Ltd, Binzhou, Shandong 256500, China

[d] College of Chemistry and Chemical Engineering, Jiangxi Normal University, Nanchang, Jiangxi 330022, China

[e] College of Materials Engineering, Fujian Agriculture and Forestry University, Fuzhou 350002, China

* Corresponding author. E-mail: liukun@ncu.edu.cn (K. Liu); liaogf@mail2.sysu.edu.cn (G. Liao); xuxianglan@ncu.edu.cn (X. Xu).

Content

S1. Supporting Figures

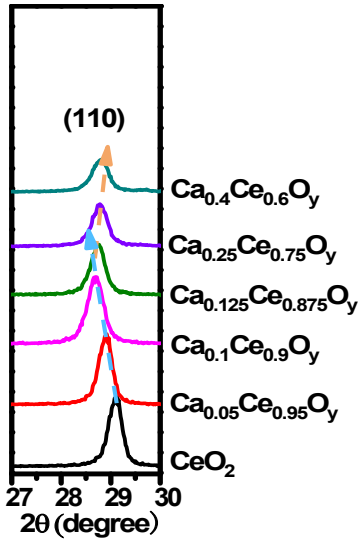

Fig. S1. The partial enlarged XRD patterns of the $Ca_xCe_{1-x}O_y$ support. When Ca ions are introduced into the CeO_2 lattice, the larger size of Ca ions compared to Ce ions leads to an increased interlayer spacing within the crystal lattice. As a result, the 2θ angle shifts towards lower angles. Furthermore, as the Ca doping concentration increases, the interlayer spacing expands further, with the greatest shift in 2θ angle occurring at a specific threshold doping level **(see Table 1).**

N_2 sorption analysis was performed to explore the textural characteristics of $Ni/Ca_xCe_{1-x}O_y$ **(Fig. S2, Table S1)**. All the catalysts displayed Type IV isotherm, along with an H3-type hysteresis loop in the relative pressure range of 0.7-1.0, indicating the presence of interparticle piled mesopores. The average pore diameters showed a relatively increasing trend, while the mean pore volumes decreased due to the

introduction of calcium. Generally, all these samples exhibited relatively similar values; therefore, it was a reasonable deduction to infer that variations in surface area did not substantially impact the catalysts' performance.

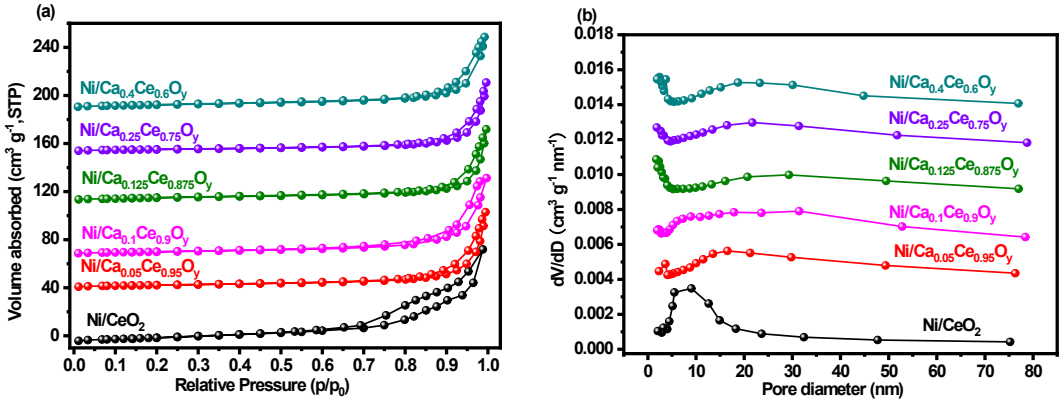

Fig. S2. (a) N_2 sorption isotherms and (b) pore-size distributions profiles of the $Ni/Ca_xCe_{1-x}O_y$ catalysts. All these samples exhibited relatively similar values, and the variations in surface area did not substantially impact the catalysts' performance **(see Table S1)**.

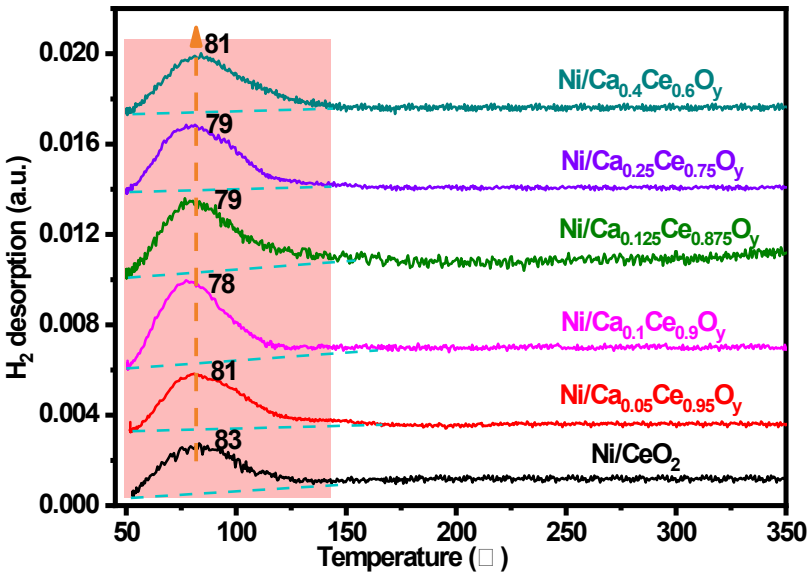

Fig. S3. The H_2 adsorption-desorption profiles on the freshly reduced $Ni/Ca_xCe_{1-x}O_y$ catalysts. The pure solid solutions can form beneficial catalytic interfaces, enhancing the dispersion of nickel **(see Table 2)**.

The crystalline phases of the fresh, reduced, and spent catalysts have been assessed through X-ray diffraction analysis. **(Fig.S4 and Table S1)**. As portrayed in **Fig. S4a**,

except diffraction peaks of $Ca_xCe_{1-x}O_y$, the characteristic diffraction peaks of NiO crystallites were detected in all $NiO/Ca_xCe_{1-x}O_y$ catalysts. In contrast, the NiO has been completely reduced to Ni among the reduced $Ni/Ca_xCe_{1-x}O_y$ catalysts, as testified by the detected metallic Ni phase **(Fig. S4b)**. And the NiO crystal sizes were calculated **(Table S2)**. The fresh NiO crystallite sizes in the $NiO/Ca_xCe_{1-x}O_y$ catalysts were found to be smaller compared to those in the fresh NiO/CeO_2 catalyst, illustrating that the incorporation of the calcium can significantly improve the synergy between NiO and the $Ca_xCe_{1-x}O_y$, although the $Ca_xCe_{1-x}O_y$ supports possessed the comparable specific surface area to the CeO_2 support **(Table S1)**. After subjecting the material to H_2 reduction, the size of metallic Ni crystallites in the reduced materials $Ni/Ca_xCe_{1-x}O_y$ (i.e.,15.5-17.7 nm) catalysts were smaller than reduced Ni/CeO_2 (i.e.,19.4 nm). The catalyst $Ni/Ca_{0.1}Ce_{0.9}O_y$, with a particle size of 15.5 nm, stood out for having the most diminutive Ni crystallite size. Compared to the freshly, reduced samples, both the spent $Ni/Ca_xCe_{1-x}O_y$ and Ni/CeO_2 catalysts exhibited similar XRD diffraction patterns. The crystallite sizes of metallic nickel in the used Ni/CeO_2 with an obvious incensement (+17.0%) in contrast to the catalyst that has undergone reduction, which showcased the aggregation and increase in size of the nickel particles throughout the entire CO_2 methanation reaction. However, there were no obvious incensement can be found the metallic Ni crystallite sizes for these used samples $Ni/Ca_xCe_{1-x}O_y$, showing that the addition of the calcium was able to hinder the agglomeration of nickel grains during the reaction. The effectiveness of a supported metal catalyst in driving reactions hinges significantly on two key factors: metal dispersion and the surface area of the active metal[1-3]. Thus, the reduced $Ni/Ca_xCe_{1-x}O_y$ catalysts have been subjected to analysis through H_2-TPD **(Fig. S3 and Table 2)**. The active metallic Ni surface areas and dispersion obeying the tendency of $Ni/Ca_{0.1}Ce_{0.9}O_y$ > $Ni/Ca_{0.125}Ce_{0.875}O_y$ > $Ni/Ca_{0.25}Ce_{0.75}O_y$ > $Ni/Ca_{0.05}Ce_{0.95}O_y$ > $Ni/Ca_{0.4}Ce_{0.6}O_y$ > Ni/CeO_2. The analysis suggests that solid solutions can form beneficial catalytic interfaces, enhancing the dispersion of nickel **(see Table S2)**.

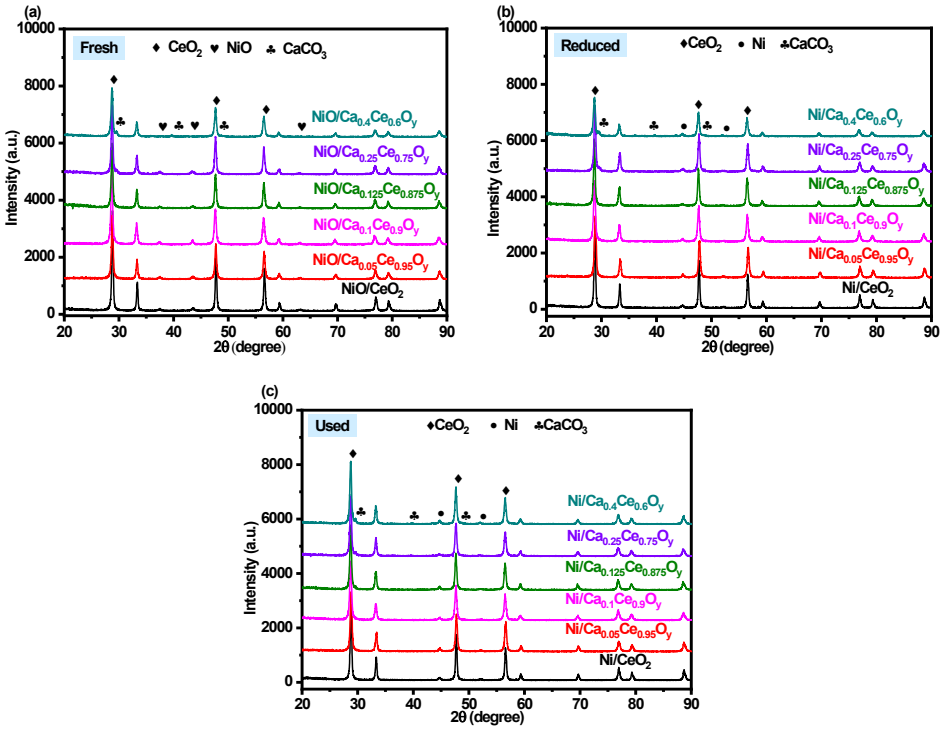

Fig. S4. X-ray diffraction patterns for the catalysts in their fresh, reduced, and spent states. The pure solid solutions can form beneficial catalytic interfaces, enhancing the dispersion of nickel, inhibiting of grain growth.

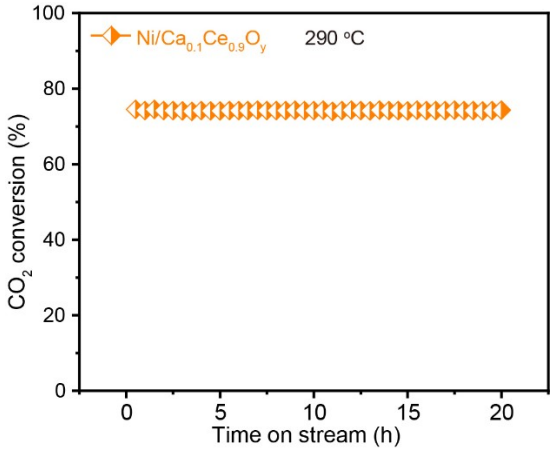

Fig. S5. Stability test diagram of $Ni/Ca_{0.1}Ce_{0.9}O_y$ catalyst at 290 °C for 20 h

S2. Supporting Tables

Table S1 Physicochemical properties of $Ni/Ca_xCe_{1-x}O_y$ catalysts.

Catalysts	S_{BET}[a]	Pore volume ($cm^3\ g^{-1}$)	Average pore size (nm)
Ni/CeO_2	21	0.12	13.8
$Ni/Ca_{0.05}Ce_{0.95}O_y$	17	0.13	23.1
$Ni/Ca_{0.1}Ce_{0.9}O_y$	18	0.11	22.0
$Ni/Ca_{0.125}Ce_{0.875}O_y$	16	0.12	24.5
$Ni/Ca_{0.25}Ce_{0.75}O_y$	16	0.10	26.5
$Ni/Ca_{0.4}Ce_{0.6}O_y$	15	0.092	25.2

Table S2 The nickel species crystallite sizes of $Ni/Ca_xCe_{1-x}O_y$ catalysts

Catalysts	Fresh catalysts	Reduced catalysts	Spent catalysts
	NiO crystallite size (nm)[a]	Ni crystallite size (nm)[a]	Ni crystallite size (nm)[a]
Ni/CeO_2	18.0	19.4	22.7
$Ni/Ca_{0.05}Ce_{0.95}O_y$	16.3	17.0	17.3
$Ni/Ca_{0.1}Ce_{0.9}O_y$	15.5	15.5	15.7
$Ni/Ca_{0.125}Ce_{0.875}O_y$	15.8	15.9	16.1
$Ni/Ca_{0.25}Ce_{0.75}O_y$	16.5	17.1	17.4
$Ni/Ca_{0.4}Ce_{0.6}O_y$	16.8	17.7	18.0

[a]Calculated from of the XRD patterns

Table S3 Quantified H_2-TPR results of the $Ca_xCe_{1-x}O_y$ support and fresh $Ni/Ca_xCe_{1-x}O_y$ catalysts.

Support	H_2 Consumption at 400-550 °C (mmol g^{-1})	Catalyst	H_2 Consumption at 200-500 °C (mmol g^{-1})	H/Ni atomic ratio
CeO_2	0.064	Ni/CeO_2	1.71	2.01
$Ca_{0.05}Ce_{0.95}O_y$	0.068	$Ni/Ca_{0.05}Ce_{0.95}O_y$	1.72	2.02
$Ca_{0.1}Ce_{0.9}O_y$	0.074	$Ni/Ca_{0.1}Ce_{0.9}O_y$	1.74	2.05
$Ca_{0.125}Ce_{0.875}O_y$	0.072	$Ni/Ca_{0.125}Ce_{0.875}O_y$	1.73	2.04
$Ca_{0.25}Ce_{0.75}O_y$	0.068	$Ni/Ca_{0.25}Ce_{0.75}O_y$	1.73	2.03
$Ca_{0.4}Ce_{0.6}O_y$	0.066	$Ni/Ca_{0.4}Ce_{0.6}O_y$	1.72	2.02

Table S4 The quantification results of oxygen properties.

Catalysts	I_{576}/I_{460} [a] ($\times10^{-2}$)	I_{1072}/I_{460} [a] ($\times10^{-2}$)
CeO_2	1.10	1.26
$Ca_{0.05}Ce_{0.95}O_y$	3.21	2.55
$Ca_{0.1}Ce_{0.9}O_y$	4.73	3.45
$Ca_{0.125}Ce_{0.875}O_y$	3.54	2.66
$Ca_{0.25}Ce_{0.75}O_y$	3.08	2.47
$Ca_{0.4}Ce_{0.6}O_y$	2.98	2.26

[a]Calculated from of the Raman results

Table S5 The quantified CO_2–TPD results on the reduced $Ni/Ca_xCe_{1-x}O_y$ catalysts.

Catalysts	$O_2^-/(O_2^-+O^{2-})$ (%)[a]	$Ce^{3+}/(Ce^{3+}+Ce^{4+})$ (%)[a]	Ca/(Ce+Ca) molar ratio[a]	Weak alkaline site amount (μmol m^{-2})[b]	Moderate alkaline site amount (μmol m^{-2})[b]	Total amount below 450 °C (μmol m^{-2})[b]
Ni/CeO_2	17.2	19.8	-	1.14	1.20	2.34
$Ni/Ca_{0.05}Ce_{0.95}O_y$	25.6	25.2	0.088	1.01	2.09	3.10
$Ni/Ca_{0.1}Ce_{0.9}O_y$	38.6	29.6	0.13	1.87	3.03	4.90
$Ni/Ca_{0.125}Ce_{0.875}O_y$	30.4	28.0	0.21	0.93	2.44	3.37
$Ni/Ca_{0.25}Ce_{0.75}O_y$	23.5	22.5	0.43	1.15	1.86	3.01
$Ni/Ca_{0.4}Ce_{0.6}O_y$	21.9	21.4	0.78	1.07	1.67	2.74

[a]Measured by XPS.

[b]Measured by CO_2-TPD.

S3. Referees

[1] Liu, K.; Xu, X.; Xu, J.; Fang, X.; Liu, L.; Wang, X., *J. CO_2 Util.* **2020,** *38*, 113-124.

[2] Xu, X.; Liu, L.; Tong, Y.; Fang, X.; Xu, J.; Jiang, D.; Wang, X., *ACS Catal.* **2021,** *11*, 5762-5775.

[3] Zhang, Z.; Tong, Y.; Fang, X.; Xu, J.; Xu, X.; Wang, X., *Fuel* **2022,** *316*, 123191.